HHS Public Access

Author manuscript

J Invest Dermatol. Author manuscript; available in PMC 2013 October 01.

Published in final edited form as:

J Invest Dermatol. 2013 April ; 133(4): 1052–1062. doi:10.1038/jid.2012.402.

The TWEAK Receptor Fn14 is a Novel Therapeutic Target in Melanoma: Immunotoxins Targeting Fn14 Receptor for Malignant Melanoma Treatment

Hong Zhou[1], **Suhendan Ekmekcioglu**[2], **John W. Marks**[1], **Khalid A. Mohamedali**[1], **Kaushal Asrani**[3], **Keeley K. Phillips**[3], **Sharron A.N. Brown**[3], **Emily Cheng**[3], **Michele B. Weiss**[4], **Walter N. Hittelman**[1], **Nhan L. Tran**[5], **Hideo Yagita**[6], **Jeffrey A. Winkles**[3,*], and **Michael G. Rosenblum**[1,*]

[1]Department of Experimental Therapeutics, UT M.D. Anderson Cancer Center, Houston, TX, 77030

[2]Department of Melanoma Medical Oncology, UT M.D. Anderson Cancer Center, Houston, TX, 77030

[3]Departments of Surgery and Physiology, Center for Vascular and Inflammatory Diseases, and the Marlene and Stewart Greenebaum Cancer Center, University of Maryland School of Medicine, Baltimore, MD, 21201

[4]Department of Cancer Biology and Kimmel Cancer Center, Thomas Jefferson University, Philadelphia, Pennsylvania, 19107

[5]The Translational Genomics Research Institute, Phoenix, AZ, 85004

[6]Department of Immunology, Juntendo University School of Medicine, Tokyo, Japan

Abstract

Fn14, the cell surface receptor for TWEAK, is over-expressed in various human solid tumor types and can be a negative prognostic indicator. We detected Fn14 expression in ~60% of the melanoma cell lines we tested, including both B-Raf WT and B-Raf^{V600E} lines. Tumor tissue microarray analysis indicated that Fn14 expression was low in normal skin but elevated in 173/190 (92%) of primary melanoma specimens and in 86/150 (58%) of melanoma metastases tested. We generated both a chemical conjugate composed of the rGel toxin and the anti-Fn14 antibody ITEM-4 (designated ITEM4-rGel) and a humanized, dimeric single-chain antibody of ITEM-4 fused to rGel (designated hSGZ). Both ITEM4-rGel and hSGZ were highly cytotoxic to a panel of different melanoma cell lines. Mechanistic studies showed that both immunotoxins

Correspondence to: Michael G. Rosenblum, Ph.D., Department of Experimental Therapeutics, M. D. Anderson Cancer Center, Unit 1950, 1515 Holcombe Boulevard, Houston, TX, 77030, mrosenbl@mdanderson.org; Phone: 713-792-3554, Jeffrey A. Winkles, Ph.D., Departments of Surgery and Physiology, 800 West Baltimore Street, Room 320, University of Maryland School of Medicine, Baltimore, MD, 21201, jwinkles@som.umaryland.edu; Phone: 410-706-8172; FAX: 410-706-8234.
*Co-Corresponding Authors.

Conflict of Interest

Michael G. Rosenblum is the co-inventor of patents covering this area.

induced melanoma cell necrosis. Also, these immunotoxins could up-regulate the cellular expression of Fn14 and trigger cell signaling events similar to the Fn14 ligand TWEAK. Finally, treatment of mice bearing human melanoma MDA-MB-435 xenografts with either ITEM4-rGel or hSGZ showed significant tumor growth inhibition compared to controls. We conclude that Fn14 is a novel therapeutic target in melanoma and the hSGZ construct appears to warrant further development as a novel therapeutic agent against Fn14-positive melanoma.

Keywords

Melanoma; Fn14; targeted therapeutics

Introduction

Metastatic melanoma has a poor prognosis, with the median survival for patients with stage IV disease ranging from 8 to 18 months (Balch *et al.*, 2009). The standard treatment regimens (DTIC or IL-2) provide only 15–25% response rates (Tsao *et al.*, 2004). Recently, ipilimumab, an antibody to cytotoxic T-lymphocyte antigen-4 (Sondak *et al.*, 2011), and the B-RAF^{V600E} inhibitor vemurafenib (Flaherty *et al.*, 2011) were approved by the FDA for treatment of unresectable or metastatic melanoma. Although there are a number of new agents and strategies under development, few achieve greater response rates (Ascierto *et al.*, 2010;Hocker *et al.*, 2008). An effective treatment strategy employing novel therapeutic approaches for advanced melanoma thus remains a critical imperative.

TWEAK and Fn14 are a TNF superfamily ligand-receptor pair involved in inflammation, oncogenesis, tumor invasion, migration, survival and resistance to chemotherapy (Burkly *et al.*, 2007;Winkles, 2008). Fn14 is expressed at relatively low levels in normal tissues, but is dramatically elevated locally in injured tissues where it plays a role in tissue remodeling (Winkles, 2008). In addition, Fn14 is highly expressed in breast (Willis *et al.*, 2008) and brain (Tran *et al.*, 2006) tumors and appears to play a role in the invasive potential of those diseases. The Fn14 gene has been shown to be overexpressed in numerous other tumor types (Culp *et al.*, 2010). The correlation between increased Fn14 expression and higher tumor grade and/or poor prognosis has been documented in brain (Tran *et al.*, 2003;Tran *et al.*, 2006), breast (Willis *et al.*, 2008), esophageal (Watts *et al.*, 2007;Wang *et al.*, 2006), prostate (Huang *et al.*, 2011), gastric (Kwon *et al.*, 2012) and bladder (Als *et al.*, 2007) cancer.

The functional relevance of this pathway in oncology suggests that an agent targeted to this pathway might be a potent cancer therapeutic (Winkles, 2008;Michaelson and Burkly, 2009). Several approaches targeting Fn14 in preclinical models have been explored (Culp *et al.*, 2010;Michaelson *et al.*, 2011;Zhou *et al.*, 2011). We previously reported that the antibody-toxin conjugate ITEM4-rGel targeting Fn14 showed significant growth inhibiting effects against numerous tumor cell lines *in vitro* and long-term growth suppression in a human bladder tumor xenograft model (Zhou *et al.*, 2011). These studies clearly suggest that therapeutic targeting of the TWEAK/Fn14 pathway represents a novel modality to inhibit tumor growth.

rGel is a type I ribosome-inactivating toxin lacking the ability to efficiently bind to the cell surface or internalize into mammalian cells (Rosenblum *et al.*, 1995) making this an excellent payload for targeted therapy approaches. Phase 1 clinical studies of an rGel immunoconjugate containing the anti-CD33 antibody HuM195 have shown limited antigenicity and no vascular leak issues with rGel even after repeated administration (Borthakur, Rosenblum, *et al*, submitted for publication). For this study, we further characterized the properties of the ITEM4-rGel conjugate described previously (Zhou *et al.*, 2011)and generated a new construct consisting of a humanized, dimeric single-chain antibody of ITEM-4 fused to rGel (designated hSGZ). Here, we present tissue microarray IHC data which identifies Fn14 as a novel therapeutic target for melanoma. In addition, we evaluated the cytotoxic efficacy of the ITEM4-rGel and hSGZ immunotoxins against a panel of melanoma cell lines *in vitro* and against MDA-MB-435 melanoma cells *in vivo*.

Results

Fn14 expression in melanoma cell lines and tumors

Fn14 expression was not detected in normal melanocytes, but it was detected in 20 of 23 melanoma cell lines tested regardless of the tumor stage which the melanoma lines represent (Fig. 1A). The B-Raf kinase has been shown to represent an important target in melanoma (Curtin *et al.*, 2005;Davies *et al.*, 2002). Fn14 expression appeared to be independent of B-Raf gene status in this panel of melanoma cell lines (Fig. 1A). We then examined a microarray composed of 40 human melanoma cell lines by IHC (Supplementary Table 1). Compared with the normal human epidermal melanocyte line NHEM-2311, Fn14 was found to be overexpressed in ~60% of the lines tested. The intensity of protein expression was slightly higher in the cell lines representing the radial growth phase (RGP). Representative images from the melanoma cell line microarray staining are shown in Fig. 1B. Fn14 expression on the melanoma cell surface was confirmed using flow cytometry (Supplementary Fig.1).

We next investigated Fn14 protein expression levels using IHC analysis on a melanoma progression tumor tissue microarray (TMA) consisting of 462 tissue cores assembled to reflect samples of tumors from each step in melanocytic tumor progression. A semiquantitative scoring system of 0 to 3 for expression levels of protein was used to reflect the staining intensity in tumor cells as illustrated in Fig. 1C. As shown in Table 1, 173/190 (92%) of primary melanoma specimens and 86/150 (58%) of melanoma metastases specimens scored positive for Fn14. Interestingly, Fn14 expression was also detected in benign nevi and was elevated in 103/122 (84%) of these samples (Table 1). There was no significant difference between individual tumor stages for Fn14 expression in this TMA. Importantly, only 19% (87/462) of the melanoma samples were negative for Fn14 expression. Fn14 expression, presented here, was scored exclusively for the tumor cell protein expression rather than stroma or immune cells residing in the tumor environment. Additionally, we did not detect Fn14 staining in primary melanocytes or tissue samples.

Immunotoxin construction, expression and purification

We modeled a single-chain version of the ITEM4-rGel immunotoxin (Zhou *et al.*, 2011) by isolating RNA from hybridoma cells expressing the ITEM-4 antibody, preparing cDNA, and amplifying the cDNA encoding murine IgG V_H and V_L regions. The V_H and V_L domains were tethered by a flexible 218 linker (Whitlow *et al.*, 1993) to produce scFv fragments in either V_H-V_L or V_L-V_H orientations. The initial rGel-based immunotoxins consisted of a flexible L linker (GGGGS) tethering the COOH terminus of scFvIT4 or $_h$scFvIT4 to the native rGel NH_2 terminus. To determine whether the relative orientation of V_H and V_L domains impacted the cytotoxic effect on Fn14-expressing tumor cells, the monovalent immunotoxins were constructed with V_H-V_L and V_L-V_H formats. To develop Fn14-targeted immunotoxins more suitable for clinical use, a humanized single-chain version of ITEM-4 (designated $_h$scFvIT4, Supplementary Fig. 2) specific for Fn14 was successfully produced and characterized. Using $_h$scFvIT4 and rGel toxin, we next engineered a bivalent immunotoxin (hSGZ) by adding a COOH-terminal dimerization domain (bZIP) (Carrillo *et al.*, 2010). Illustrations of the immunotoxin constructs are shown in Fig. 2A. Following purification, all the rGel-based immunotoxins migrated on SDS-PAGE at the expected molecular weights of ~55 kDa for monovalent immunotoxins and ~120 kDa for bivalent immunotoxin (Fig. 2B).

Binding of immunotoxins to Fn14

The binding of ITEM-4, scFvs and immunotoxins to recombinant Fn14 extracellular domain was assessed by surface plasmon resonance (BIAcore) analysis. We found that ITEM-4, scFvIT4, and $_h$scFvIT4 bound to Fn14 with similar equilibrium dissociation constants (K_ds) of ~1.14, 1.19, and 6.25 nmol/L, respectively (Fig. 2C). The immunotoxins ITEM4-rGel, scFvIT4/rGel (V_H-V_L), scFvIT4/rGel (V_L-V_H), hSGZ (monomer) and hSGZ (dimer) bound to Fn14 with equilibrium dissociation constants (K_ds) of 2.5, 1.08, 2.3, 2.5 and 1.4 nmol/L, respectively (Fig. 2C). Purified rGel did not bind to Fn14 in this assay. Both immunotoxins showed specific binding to MDA-MB-435 cells compared to the background of binding to Fn14-deficient mouse embryonic fibroblasts (MEF 3.5 −/−) in an enzyme-linked immunosorbent assay (ELISA)-based binding assay (Supplementary Fig. 3A).

Conversion into a bivalent format improves the cytotoxic effects of scFvIT4/rGel

We investigated whether ITEM4-rGel and the scFvIT4/rGel-based fusion proteins had similar cytotoxicity against various melanoma cell lines. To quantitatively compare the cytotoxicity of bivalent and monovalent formats, dose-dependent growth inhibition curves were established on MDA-MB-435 cells (Fig. 2D). An IC_{50} value of 0.006 nmol/L was obtained for ITEM4-rGel. IC_{50} values of 12.0, 3.6 and 18.3 nmol/L were obtained for scFvIT4/rGel (V_H-V_L), scFvIT4/rGel (V_L-V_H) (Fig. 2D) and hSGZ (monomer) (Supplementary Fig. 3B), respectively. An IC_{50} value of 0.008 nmol/L was calculated for hSGZ dimer (Fig. 2D and Supplementary Fig. 3B). Thus, a 2287-fold reduction in IC_{50} value was achieved by converting monomeric hSGZ into homodimeric, bivalent hSGZ. Unless otherwise specified, hSGZ refers to the dimeric construct.

ITEM4-rGel and hSGZ demonstrated significant cytotoxicity against melanoma cell lines (IC_{50} ranged from 0.1 pmol/L-1.1 nmol/L) and they were 2.2 to 2.8 $\times 10^5$ fold more potent

than free rGel (Supplementary Table 2). By comparison, the cytotoxic effects of these immunotoxins on Fn14-negative MEF3.5 −/− cells was similar to that of free rGel (Supplementary Table 2). As shown in Fig. 2E, pre-incubation with 1 μmol/L ITEM-4 for 4 h shifted the ITEM4-rGel and hSGZ induced cytotoxicity to that of the rGel curve in WM35 cells.

Cellular uptake of immunotoxins

Immunofluorescence staining was done on MDA-MB-435 and MEF 3.5−/− cells after exposure to the immunotoxins. As shown in Fig. 2F, the rGel moiety (green) of both immunotoxins was observed primarily in the cytosol of MDA-MB-435 cells. Internalization did not occur in MEF 3.5−/− cells (data not shown).

Mechanistic studies of immunotoxin cytotoxic effects

Immunotoxins did not induce apoptosis or autophagy when added to Fn14-positive melanoma cells (Supplementary Fig. 4). To assess whether necrotic cell death was induced, we performed a PI exclusion assay which investigates the early loss of plasma membrane integrity that occurs during classical necrosis (Do *et al.*, 2003). MDA-MB-435 and AAB-527 cells displayed an increasing loss of plasma membrane integrity after treatment with ITEM4-rGel or hSGZ but not treatment with ITEM-4 or rGel (Fig. 3A). In contrast, immunotoxins did not induce necrosis when added to MEF3.5−/− cells (Supplementary Fig. 4C). For further confirmation of a necrotic response, the lactate dehydrogenase (LDH) release assay was used to measure cell lysis (Do *et al.*, 2003). Immunotoxin-induced LDH release was found to be both time- and dose-dependent for both cell lines studied; however, treatment with ITEM-4 and rGel did not induce LDH release in this assay (Fig. 3B).

A common event in numerous forms of cell death is mitochondrial outer membrane permeabilization (MOMP) which results in escape of mitochondrial proteins that are toxic within the cytosol, then a rapid decline in ATP production and the generation of reactive oxygen species (ROS) (Kroemer and Martin, 2005). We also found that exposure of MDA-MB-435 and AAB-527 cells to ITEM4-rGel and hSGZ but not ITEM-4 or rGel resulted in mitochondrial membrane depolarization using the mitochondrial dye JC-1 (Fig. 3C). This finding indicates that the immunotoxins may promote ROS release, which could contribute to cell death induced by these constructs.

The ITEM-4 antibody and derivative immunotoxins can up-regulate Fn14 expression and activate the NF-κB pathway

It has been reported that TWEAK treatment of human glioma (Tran *et al.*, 2006) and prostate (Huang *et al.*, 2011) tumor cells increases Fn14 gene expression. Since ITEM-4 has agonistic activity (Nakayama *et al.*, 2003) we considered the possibility that the ITEM4-based immunotoxins might actually increase expression of their cell surface target. ITEM-4 treatment increased Fn14 expression in all cell lines tested (Fig. 4A and Supplementary Fig. 5A, B). Since Fn14 is an NF-κB target gene (Tran *et al.*, 2006), we tested if ITEM-4 could activate the NF-κB pathway using a HEK293/NFκB-luc/Fn14 luciferase reporter cell line. ITEM-4, but not isotype-matched control IgG, dose-dependently resulted in induction of the NF-κB pathway reporter gene (Fig. 4B). Consistent with this data, we found that ITEM4-

rGel and hSGZ can induce both the classical (not shown) and alternative NF-κB signaling pathways as well as Fn14 expression after treatment of MDA-MB-435 cells (Fig. 4C and 4D) and AAB-527 cells (Supplementary Fig. 5C), similar to the effect observed upon treatment with ITEM-4 and TWEAK. We also detected increase Fn14 levels on the melanoma cell surface after immunotoxin treatment (Supplementary Fig. 5E). Finally, ITEM4-rGel and hSGZ can also induce expression of additional NF-κB-regulated genes, including IL-8 and TNF-α (Supplementary Fig. 5D). Taken together, the data indicate that the ITEM4-rGel and hSGZ exhibit agonistic activity, including activation of the NF-κB signaling pathway and induction of Fn14, IL-8 and TNFα production, analogous to the effects of TWEAK.

hSGZ exhibited comparative *in vivo* tumor growth inhibition activity to ITEM4-rGel

We next examined the effect of immunotoxins on the growth of established human melanoma (MDA-MB-435-Luc) xenografts assessed by either caliper measurement or bioluminescence imaging (BLI). Significant tumor growth inhibition was observed at doses of 30 or 60 mg/kg of the ITEM4-rGel (Fig. 5A and Supplementary Fig. 6B) and 25 or 50 mg/kg of the hSGZ construct (Fig. 5B and Supplementary Fig. 6D) compared to saline-treated controls ($P < 0.005$). Mice treated with 60 mg/kg ITEM-4 also had less tumor growth relative to the saline control; however, this difference bordered on statistical significance ($P = 0.049$). The representative BLI images of the tumors on selected days clearly demonstrated the antitumor properties of the ITEM4-rGel (Supplementary Fig. 6A) and hSGZ (Fig. 5C). We also found that hSGZ treatment upregulated Fn14 expression *in vivo* as assayed by Western blot analysis of tumor tissues (Fig. 5D). Immunofluorescence staining confirmed that ITEM4-rGel and hSGZ localized specifically in tumor tissue and no nonspecific staining was observed in tumors after administration of ITEM-4 and saline detected by anti-rGel antibody (Fig. 5E). This suggests that the ITEM4-rGel and hSGZ can target tumor cells overexpressing Fn14 *in vivo*. Toxicity was monitored by frequent body weight measurements in groups of mice treated with ITEM4-rGel or hSGZ. Body weights showed less than a 20% change in any of the treated mice over the duration of the experiment for ITEM4-rGel (Supplementary Fig. 6C) and hSGZ (Supplementary Fig. 6E) administration.

Discussion

This study identifies Fn14 as a potential new target for melanoma therapy. We first explored the expression characteristics of Fn14 in a large set of melanoma cell lines representing various stages of disease progression. Our results showed that while increased expression of Fn14 in melanoma cell lines is suggestive of a link to melanoma, even more notable is that in some melanoma cell lines (such as WM35 P1.N1, WM35 P2.N1) there appears to be a link between Fn14 expression and tumor progression. Nevi may further progress to melanoma or can regress by differentiating to cell types that have been histopathologically defined as (non malignant) Schwann cells (Clark, Jr. *et al.*, 1984). Interestingly, Fn14 was expressed at a similar frequency in benign nevi and in primary melanomas, but with a lower frequency in metastatic melanomas suggesting that it is upregulated in early melanoma

tumorigenesis. The high percentage of Fn14 expression in melanoma prompted us to develop the Fn14-targeted immunotoxins as anti-melanoma therapeutic agents.

We constructed different formats of immunotoxins and all of them showed high binding to Fn14. The conversion of monovalent hSGZ immunotoxin into a bivalent format by adding a COOH-terminal dimerization domain dramatically enhanced the potency of this construct *in vitro* (Fig. 2D and Supplementary Fig. 3B), suggesting an effect of higher order cross-linking of Fn14 molecules on the cell surface induced by bivalent binding.

Cell death caused by Fn14-targeted immunotoxins could be the result of a combination of activation of the intrinsic cytotoxicity related to the Fn14 pathway (Michaelson and Burkly, 2009) and the inhibition of protein synthesis by the rGel toxin. We previously demonstrated that the ITEM4-rGel immunotoxin killed T-24 bladder tumor cells through an apoptotic mechanism with release of HMGB1 protein (Zhou *et al.*, 2011). However, the cytotoxic effects of ITEM4-rGel and hSGZ on melanoma cells occurred through a cellular necrosis mechanism and involved LDH release. Taken together, these data suggest that Fn14-targeted immunotoxins can induce cell death through different mechanisms and the effects appear to be cell type-dependent. The necrotic cell death mechanism observed after melanoma cell exposure to the Fn14-targeted immunotoxins may also be the result of the well-known intrinsic resistance of these cells to apoptosis (Soengas and Lowe, 2003).

In general, the efficacy of antibody-based therapies can be hampered as the tumor cells adopt defensive tactics such as shedding of the target antigen/receptor and masking to escape immune surveillance. Target antigen/receptor expression may also be down-regulated *in vivo* due to therapy with other agents. We found that Fn14 expression was up-regulated by ITEM-4 treatment. This effect was also observed with the natural Fn14 ligand TWEAK and the immunotoxins. Consistent with our *in vitro* results, Fn14 expression in xenograft tumors was up-regulated by hSGZ administration (Fig.5D). We also showed that, like TWEAK, Fn14-targeted immunotoxins are capable of inducing NF-κB pathway activation. Signaling by the TWEAK/Fn14 axis appears to exert either pro-tumorigenic or anti-tumorigenic effects depending on the particular microenvironment (Michaelson and Burkly, 2009;Winkles, 2008). It is important to note that no enhancement in tumor growth was observed following ITEM-4 treatment in our xenograft models. This result is consistent with prior data indicating that administration of TWEAK resulted in dramatic reduction in tumor growth in xenograft models (Michaelson *et al.*, 2011). ITEM4-rGel was found to be slightly more potent than hSGZ in the xenograft model (Fig. 5A and B, ITEM4-rGel 30mg/kg treated group *vs* hSGZ 50 mg/kg treated group). The better potency observed with ITEM4-rGel could be due to the longer half-life of the larger IgG conjugate *in vivo* (Zalevsky *et al.*, 2010), antibody-dependent cellular cytotoxicity (ADCC) of ITEM-4 (Nakayama *et al.*, 2003) and a more efficient agonistic activity of the IgG construct in this specific setting. Given the cross-species reactivity of ITEM-4 to mouse Fn14, the toxicity of ITEM4-rGel or hSGZ on non-tumor tissues *in vivo* was found to be minimal and this may be reflective of expected toxicity in patients.

The abundant overexpression of Fn14 in melanoma makes it an attractive cell surface target for agents such as immunotoxins. hSGZ, the humanized counterpart of ITEM4-rGel, has a

unique cytotoxicity to melanoma and these findings, together with its *in vivo* anti-tumor efficacy, suggest that hSGZ warrants further development as a novel therapeutic agent against Fn14-positive melanoma.

Materials and Methods

Cell lines and reagents

Human melanoma cell lines (WM3211, Sbcl2, WM1346, WM1361A, WM1366, WM793, WM983A, MeWo, WM46, A375, WM983B, SK-MEL-3, SK-MEL-24, SK-MEL-28, SK-MEL-32, WM35, WM35P2N1, SB2, SK-MEL-1, SK-MEL-5) were maintained in RPMI 1640 medium (HyClone, Logan, UT). Melanoma cell lines A375M, AAB-527 and Fn14-deficient mouse embryonic fibroblasts (MEF 3.5−/−) were maintained in DMEM (HyClone). All medium contained 10% FBS. The luciferase-expressing human melanoma cell line MDA-MB-435-Luc was derived from MDA-MB-435 cells as previously reported (Murray *et al.*, 2003). The murine IgG2b/κ monoclonal antibody ITEM-4 directed against human and mouse Fn14 receptor (Nakayama *et al.*, 2003) and the generation of immunoconjugate ITEM4-rGel have been described previously (Zhou *et al.*, 2011). Recombinant human TWEAK was purchased from R&D Systems (Minneapolis, MN).

Melanoma cell line microarray, TMA and immunohistochemistry

A human melanoma cell line microarray was established at M.D. Anderson Cancer Center (MDACC). The melanocytic tumor progression TMA was designed to provide samples of tumors from each step in melanocytic tumor progression (Nazarian *et al.*, 2010). The TMA contains 462 tissue cores from 169 patients, consisting of benign nevi (122 cores from 35 patients), primary cutaneous melanomas (190 cores from 59 patients), melanoma metastases to lymph nodes (60 cores from 29 patients), and melanoma metastases to visceral organs (90 cores from 46 patients). Acral, mucosal, and uveal melanomas were excluded from this TMA (Nazarian *et al.*, 2010). Immunohistochemical analysis for Fn14 was performed as previously described using 2.5 μg/ml of the Fn14 monoclonal antibody P4A8 and an isotype matched murine IgG as control (Tran *et al.*, 2003). Immunolabeling was scored separately for 2 variables; first, for number of positive melanoma cells; second, for the overall intensity of immunoreactivity of the positive cells. Scoring for number of positive tumor cells was defined as follows: 0, <5% positive cells; 1, 5–25% positive cells; 2, >25– 75% positive cells; 3, > 75% positive cells. Intensity scoring was defined as follows; 0, no staining; 1, light staining; 2, moderate staining and 3, intense staining. The slides were independently interpreted by 2 readers without knowledge of the clinical data. Any discrepancies in scores were subsequently reconciled.

In vitro studies

The following methods are described in Supplementary Materials and Methods: cloning and humanization of single-chain Fv (scFv); plasmid construction; protein expression in *E. coli*; isolation and purification of fusion immunotoxins; surface plasmon resonance assay (Brown *et al.*, 2006); ELISA (Cao *et al.*, 2009) and internalization analyses (Zhou *et al.*, 2011); reticulocyte lysate *in vitro* translation assay (Hale, 2001); *in vitro* cytotoxicity assay (Zhou *et al.*, 2011); flow cytometry analysis (Zhou *et al.*, 2011); PI exclusion assay (Do *et al.*,

2003); LDH release assay; mitochondrial membrane depolarization assay; apoptosis assay; Western blot analysis; and NF-κB pathway luciferase reporter assay (Brown *et al.*, 2010).

In vivo efficacy studies

Animal procedures were conducted according to a protocol approved by the AALAC-approved Animal Care and Use Facility at MDACC. Female BALB/c nude mice (Harlan Sprague Dawley Inc, Indianapolis, IN), 8 weeks old, were injected (hind flank) subcutaneously with MDA-MB-435-LUC cells (1×10^7 cells per mouse; suspended in 100 μL of PBS mixed with 100 μL BD Matrigel). Once tumors reached a mean volume of ~200 mm^3, animals (5 mice per group) were treated (*i.v.* via tail vein) with PBS, ITEM-4 or with immunotoxins. Animals were monitored and tumors were measured every 2–3 days. Data are presented as mean tumor volume (mm^3) ± SD.

BLI

In vivo BLI was conducted using the IVIS100 system with Living Image acquisition and analysis software (Caliper Life Sciences, Hopkinton, MA). Anesthetized mice were *i.p.* injected with 75 mg/kg D-luciferin (Gold Biotechnology, Inc., St.Louis, MO) and imaged for 10 minutes after luciferin injection.

Localization of ITEM4-rGel and hSGZ in tumor tissue

Twenty-four hours after *i.v.* injection of ITEM-4, ITEM4-rGel or hSGZ, mice were sacrificed and tumor samples were collected and frozen immediately for sectioning. Localization of ITEM4-rGel and hSGZ in tumor tissues was assessed as previously described (Zhou *et al.*, 2011).

Statistical analysis

A number of statistical methods were employed for the analysis of the microarray data. Cohen's Kappa coefficient was estimated to assess the degree of agreement between duplicate readings for the same sample. In addition, Bowker's test of symmetry was applied to the analyses. To determine the relationship between Fn14 readings and disease stages, the Fn14 percentages or intensity scores were treated as ordinal responses and an ordinal regression model accounting for repeated measurements within each sample was used to fit the Fn14 scores. All computations including Chi-squared tests were performed in SAS v9.2. P values were obtained using 1-tailed t test with 95% confidence interval for evaluation of the statistical significance compared with the controls in the animal studies. $P < 0.05$ was considered statistically significant.

Supplementary Material

Refer to Web version on PubMed Central for supplementary material.

Acknowledgments

We thank Dr. Lyn Duncan (Massachusetts General Hospital, Boston, MA) for providing the Melanoma Progression TMA.

Funding:

This work was conducted, in part, by the Clayton Foundation for Research (MGR), National Institutes of Health (NIH) grants R01 NS055126 (JAW), R01 CA130940 (NLT) and T32 HL007698 (E.C.) and Department of Defense Concept Award BC086135 (JAW). Michele's work was performed in Dr. Andrew E. Aplin's lab under the funding of NIH grant CA125103. STR DNA fingerprinting of our melanoma cell lines was supported by MDACC Institutional Core Grant NIH CA016672.

Abbreviation list

TNF	Tumor necrosis factor
TWEAK	TNF-like weak inducer of apoptosis
Fn14	fibroblast growth factor -inducible protein 14
rGel	recombinant gelonin

References

Als AB, Dyrskjot L, von der MH, Koed K, Mansilla F, Toldbod HE, Jensen JL, Ulhoi BP, Sengelov L, Jensen KM, Orntoft TF. Emmprin and survivin predict response and survival following cisplatin-containing chemotherapy in patients with advanced bladder cancer. Clin Cancer Res. 2007; 13:4407–4414. [PubMed: 17671123]

Ascierto PA, Streicher HZ, Sznol M. Melanoma: a model for testing new agents in combination therapies. J Transl Med. 2010; 8:38. [PubMed: 20406483]

Balch CM, Gershenwald JE, Soong SJ, Thompson JF, Atkins MB, Byrd DR, Buzaid AC, Cochran AJ, Coit DG, Ding S, Eggermont AM, Flaherty KT, Gimotty PA, Kirkwood JM, McMasters KM, Mihm MC Jr, Morton DL, Ross MI, Sober AJ, Sondak VK. Final version of 2009 AJCC melanoma staging and classification. J Clin Oncol. 2009; 27:6199–6206. [PubMed: 19917835]

Brown SA, Ghosh A, Winkles JA. Full-length, membrane-anchored TWEAK can function as a juxtacrine signaling molecule and activate the NF-kappaB pathway. J Biol Chem. 2010; 285:17432–17441. [PubMed: 20385556]

Brown SA, Hanscom HN, Vu H, Brew SA, Winkles JA. TWEAK binding to the Fn14 cysteine-rich domain depends on charged residues located in both the A1 and D2 modules. Biochem J. 2006; 397:297–304. [PubMed: 16526941]

Burkly LC, Michaelson JS, Hahm K, Jakubowski A, Zheng TS. TWEAKing tissue remodeling by a multifunctional cytokine: role of TWEAK/Fn14 pathway in health and disease. Cytokine. 2007; 40:1–16. [PubMed: 17981048]

Cao Y, Marks JD, Marks JW, Cheung LH, Kim S, Rosenblum MG. Construction and characterization of novel, recombinant immunotoxins targeting the Her2/neu oncogene product: in vitro and in vivo studies. Cancer Res. 2009; 69:8987–8995. [PubMed: 19934334]

Carrillo RJ, Dragan AI, Privalov PL. Stability and DNA-binding ability of the bZIP dimers formed by the ATF-2 and c-Jun transcription factors. J Mol Biol. 2010; 396:431–440. [PubMed: 19944700]

Clark WH Jr, Elder DE, Guerry D, Epstein MN, Greene MH, Van HM. A study of tumor progression: the precursor lesions of superficial spreading and nodular melanoma. Hum Pathol. 1984; 15:1147–1165. [PubMed: 6500548]

Culp PA, Choi D, Zhang Y, Yin J, Seto P, Ybarra SE, Su M, Sho M, Steinle R, Wong MH, Evangelista F, Grove J, Cardenas M, James M, Hsi ED, Chao DT, Powers DB, Ramakrishnan V, Dubridge R. Antibodies to TWEAK receptor inhibit human tumor growth through dual mechanisms. Clin Cancer Res. 2010; 16:497–508. [PubMed: 20068083]

Curtin JA, Fridlyand J, Kageshita T, Patel HN, Busam KJ, Kutzner H, Cho KH, Aiba S, Brocker EB, LeBoit PE, Pinkel D, Bastian BC. Distinct sets of genetic alterations in melanoma. N Engl J Med. 2005; 353:2135–2147. [PubMed: 16291983]

Davies H, Bignell GR, Cox C, Stephens P, Edkins S, Clegg S, Teague J, Woffendin H, Garnett MJ, Bottomley W, Davis N, Dicks E, Ewing R, Floyd Y, Gray K, Hall S, Hawes R, Hughes J,

Kosmidou V, Menzies A, Mould C, Parker A, Stevens C, Watt S, Hooper S, Wilson R, Jayatilake H, Gusterson BA, Cooper C, Shipley J, Hargrave D, Pritchard-Jones K, Maitland N, Chenevix-Trench G, Riggins GJ, Bigner DD, Palmieri G, Cossu A, Flanagan A, Nicholson A, Ho JW, Leung SY, Yuen ST, Weber BL, Seigler HF, Darrow TL, Paterson H, Marais R, Marshall CJ, Wooster R, Stratton MR, Futreal PA. Mutations of the BRAF gene in human cancer. Nature. 2002; 417:949–954. [PubMed: 12068308]

Do TN, Rosal RV, Drew L, Raffo AJ, Michl J, Pincus MR, Friedman FK, Petrylak DP, Cassai N, Szmulewicz J, Sidhu G, Fine RL, Brandt-Rauf PW. Preferential induction of necrosis in human breast cancer cells by a p53 peptide derived from the MDM2 binding site. Oncogene. 2003; 22:1431–1444. [PubMed: 12629507]

Flaherty KT, Yasothan U, Kirkpatrick P. Vemurafenib. Nat Rev Drug Discov. 2011; 10:811–812. [PubMed: 22037033]

Hale ML. Microtiter-based assay for evaluating the biological activity of ribosomein-activating proteins. Pharmacol Toxicol. 2001; 88:255–260. [PubMed: 11393586]

Hocker TL, Singh MK, Tsao H. Melanoma genetics and therapeutic approaches in the 21st century: moving from the benchside to the bedside. J Invest Dermatol. 2008; 128:2575–2595. [PubMed: 18927540]

Huang M, Narita S, Tsuchiya N, Ma Z, Numakura K, Obara T, Tsuruta H, Saito M, Inoue T, Horikawa Y, Satoh S, Habuchi T. Overexpression of Fn14 promotes androgen-independent prostate cancer progression through MMP-9 and correlates with poor treatment outcome. Carcinogenesis. 2011; 32:1589–1596. [PubMed: 21828059]

Kroemer G, Martin SJ. Caspase-independent cell death. Nat Med. 2005; 11:725–730. [PubMed: 16015365]

Kwon OH, Park SJ, Kang TW, Kim M, Kim JH, Noh SM, Song KS, Yoo HS, Wang Y, Pocalyko D, Paik SG, Kim YH, Kim SY, Kim YS. Elevated fibroblast growth factor-inducible 14 expression promotes gastric cancer growth via nuclear factor-kappaB and is associated with poor patient outcome. Cancer Lett. 2012; 314:73–81. [PubMed: 21993017]

Michaelson JS, Amatucci A, Kelly R, Su L, Garber E, Day ES, Berquist L, Cho S, Li Y, Parr M, Wille L, Schneider P, Wortham K, Burkly LC, Hsu YM, Joseph IB. Development of an Fn14 agonistic antibody as an anti-tumor agent. MAbs. 2011; 3:362–375. [PubMed: 21697654]

Michaelson JS, Burkly LC. Therapeutic targeting of TWEAK/Fnl4 in cancer: exploiting the intrinsic tumor cell killing capacity of the pathway. Results Probl Cell Differ. 2009; 49:145–160. [PubMed: 19513634]

Murray LJ, Abrams TJ, Long KR, Ngai TJ, Olson LM, Hong W, Keast PK, Brassard JA, O'Farrell AM, Cherrington JM, Pryer NK. SU11248 inhibits tumor growth and CSF-1R-dependent osteolysis in an experimental breast cancer bone metastasis model. Clin Exp Metastasis. 2003; 20:757–766. [PubMed: 14713109]

Nakayama M, Ishidoh K, Kojima Y, Harada N, Kominami E, Okumura K, Yagita H. Fibroblast growth factor-inducible 14 mediates multiple pathways of TWEAK-induced cell death. J Immunol. 2003; 170:341–348. [PubMed: 12496418]

Nazarian RM, Prieto VG, Elder DE, Duncan LM. Melanoma biomarker expression in melanocytic tumor progression: a tissue microarray study. J Cutan Pathol. 2010; 37(Suppl 1):41–47. [PubMed: 20482674]

Rosenblum MG, Kohr WA, Beattie KL, Beattie WG, Marks W, Toman PD, Cheung L. Amino acid sequence analysis, gene construction, cloning, and expression of gelonin, a toxin derived from Gelonium multiflorum. J Interferon Cytokine Res. 1995; 15:547–555. [PubMed: 7553224]

Soengas MS, Lowe SW. Apoptosis and melanoma chemoresistance. Oncogene. 2003; 22:3138–3151. [PubMed: 12789290]

Sondak VK, Smalley KS, Kudchadkar R, Grippon S, Kirkpatrick P. Ipilimumab. Nat Rev Drug Discov. 2011; 10:411–412. [PubMed: 21629286]

Tran NL, McDonough WS, Donohue PJ, Winkles JA, Berens TJ, Ross KR, Hoelzinger DB, Beaudry C, Coons SW, Berens ME. The human Fn14 receptor gene is up-regulated in migrating glioma cells in vitro and overexpressed in advanced glial tumors. Am J Pathol. 2003; 162:1313–1321. [PubMed: 12651623]

Tran NL, McDonough WS, Savitch BA, Fortin SP, Winkles JA, Symons M, Nakada M, Cunliffe HE, Hostetter G, Hoelzinger DB, Rennert JL, Michaelson JS, Burkly LC, Lipinski CA, Loftus JC, Mariani L, Berens ME. Increased fibroblast growth factor-inducible 14 expression levels promote glioma cell invasion via Rac1 and nuclear factor-kappaB and correlate with poor patient outcome. Cancer Res. 2006; 66:9535–9542. [PubMed: 17018610]

Tsao H, Atkins MB, Sober AJ. Management of cutaneous melanoma. N Engl J Med. 2004; 351:998–1012. [PubMed: 15342808]

Wang S, Zhan M, Yin J, Abraham JM, Mori Y, Sato F, Xu Y, Olaru A, Berki AT, Li H, Schulmann K, Kan T, Hamilton JP, Paun B, Yu MM, Jin Z, Cheng Y, Ito T, Mantzur C, Greenwald BD, Meltzer SJ. Transcriptional profiling suggests that Barrett's metaplasia is an early intermediate stage in esophageal adenocarcinogenesis. Oncogene. 2006; 25:3346–3356. [PubMed: 16449976]

Watts GS, Tran NL, Berens ME, Bhattacharyya AK, Nelson MA, Montgomery EA, Sampliner RE. Identification of Fn14/TWEAK receptor as a potential therapeutic target in esophageal adenocarcinoma. Int J Cancer. 2007; 121:2132–2139. [PubMed: 17594693]

Whitlow M, Bell BA, Feng SL, Filpula D, Hardman KD, Hubert SL, Rollence ML, Wood JF, Schott ME, Milenic DE. An improved linker for single-chain Fv with reduced aggregation and enhanced proteolytic stability. Protein Eng. 1993; 6:989–995. [PubMed: 8309948]

Willis AL, Tran NL, Chatigny JM, Charlton N, Vu H, Brown SA, Black MA, McDonough WS, Fortin SP, Niska JR, Winkles JA, Cunliffe HE. The fibroblast growth factor-inducible 14 receptor is highly expressed in HER2-positive breast tumors and regulates breast cancer cell invasive capacity. Mol Cancer Res. 2008; 6:725–734. [PubMed: 18505918]

Winkles JA. The TWEAK-Fn14 cytokine-receptor axis: discovery, biology and therapeutic targeting. Nat Rev Drug Discov. 2008; 7:411–425. [PubMed: 18404150]

Zalevsky J, Chamberlain AK, Horton HM, Karki S, Leung IW, Sproule TJ, Lazar GA, Roopenian DC, Desjarlais JR. Enhanced antibody half-life improves in vivo activity. Nat Biotechnol. 2010; 28:157–159. [PubMed: 20081867]

Zhou H, Marks JW, Hittelman WN, Yagita H, Cheung LH, Rosenblum MG, Winkles JA. Development and characterization of a potent immunoconjugate targeting the Fn14 receptor on solid tumor cells. Mol Cancer Ther. 2011; 10:1276–1288. [PubMed: 21586630]

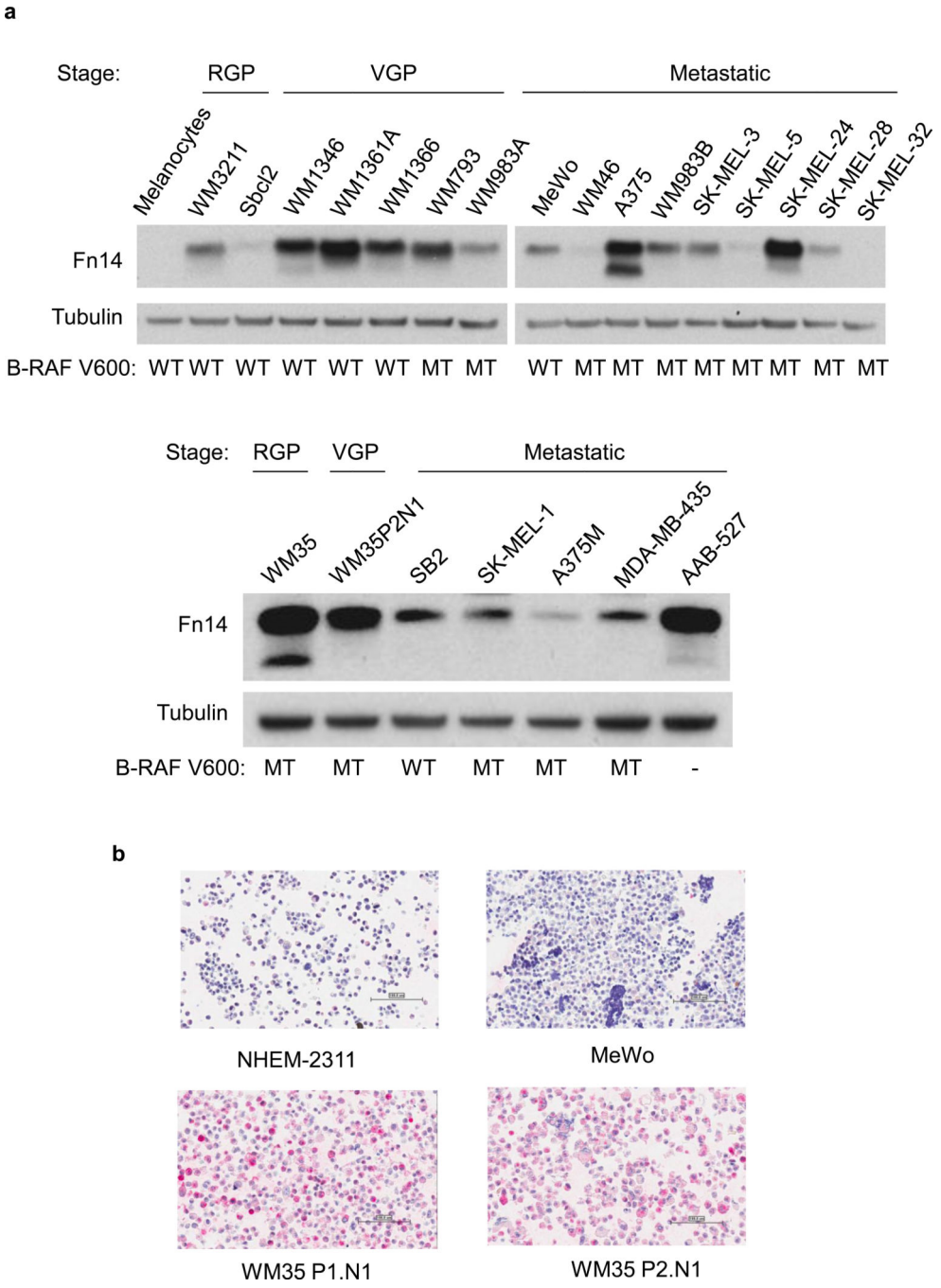

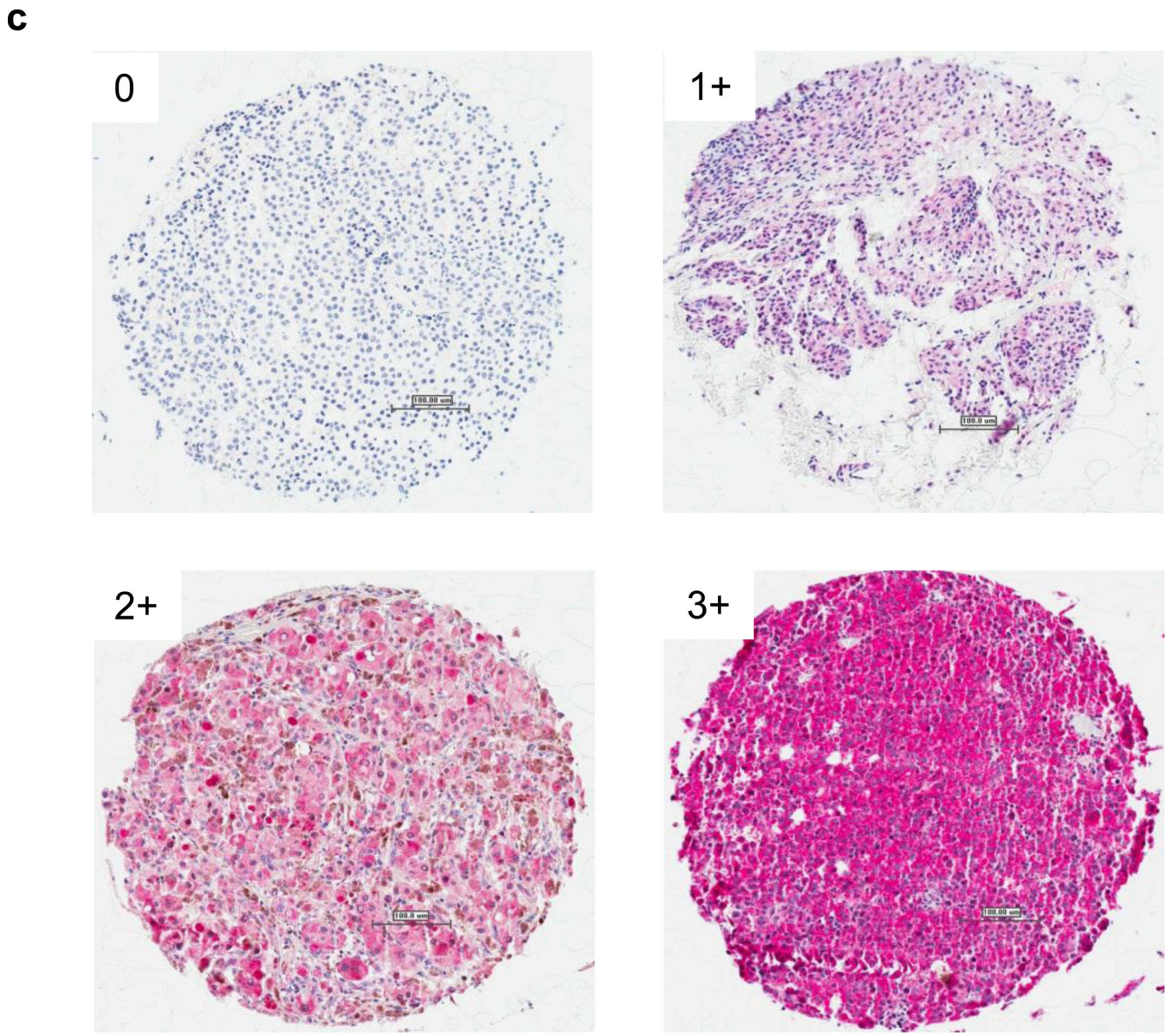

Figure 1.

Fn14 is overexpressed in melanoma cell lines and human tumor samples. **A**) Cell lines were assayed for Fn14 and tubulin levels by Western blot. B-RAF status is indicated: WT, wild type; MT, V600E mutant. Abbreviations: RGP, radial-growth phase; VGP, vertical-growth phase. **B**) Fn14 expression in melanoma cell lines was also assayed using a cell line microarray and an anti-Fn14 antibody. Images from four of the lines are shown. Scale bar = 100 μm. **C**) Paraffin sections of melanocytic tumor progression tissue microarray were immunostained with an anti-Fn14 antibody. A relative staining intensity (0 – 3+) was assigned and a melanoma specimen representing each intensity level is presented. Scale bar = 100 μm.

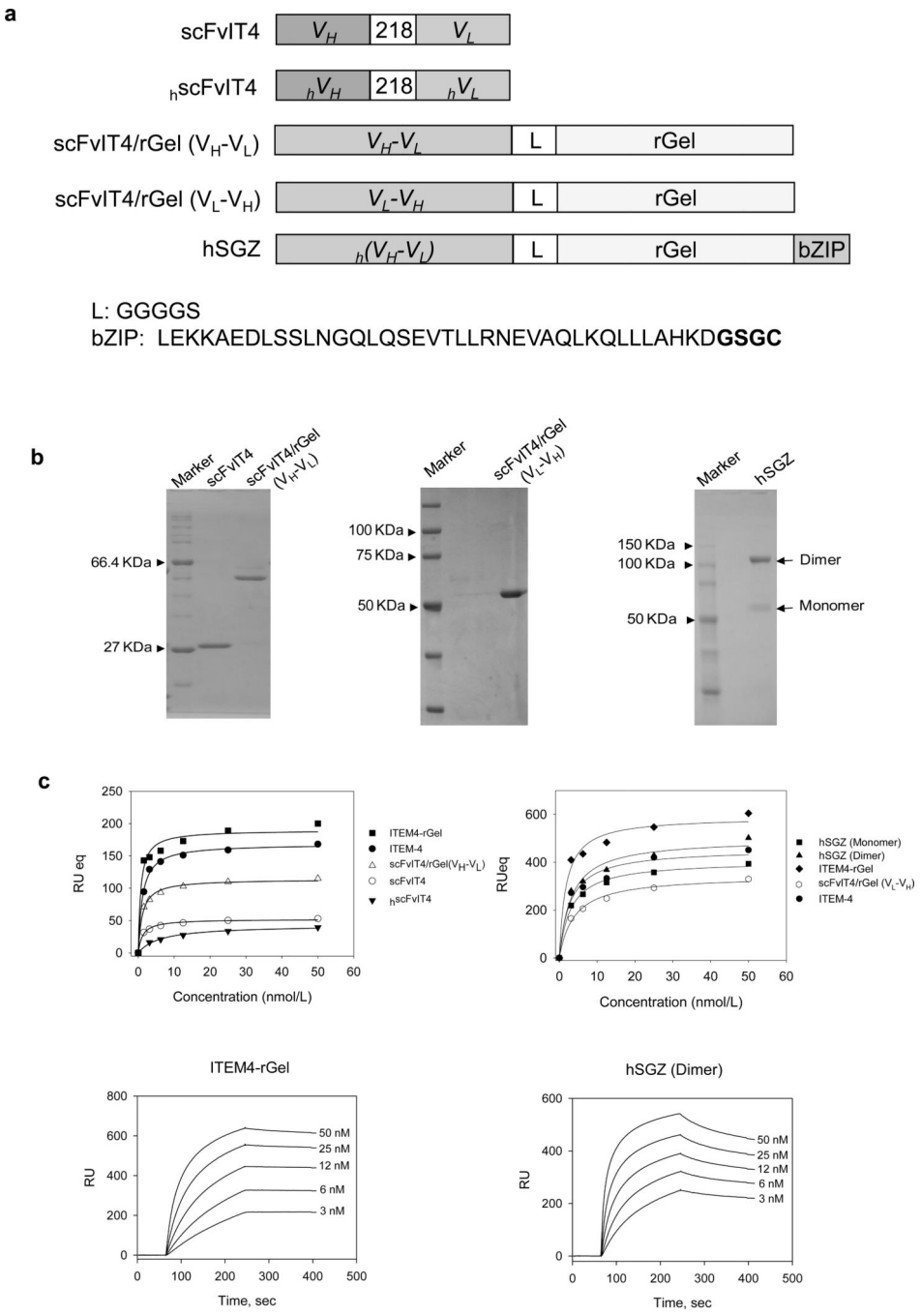

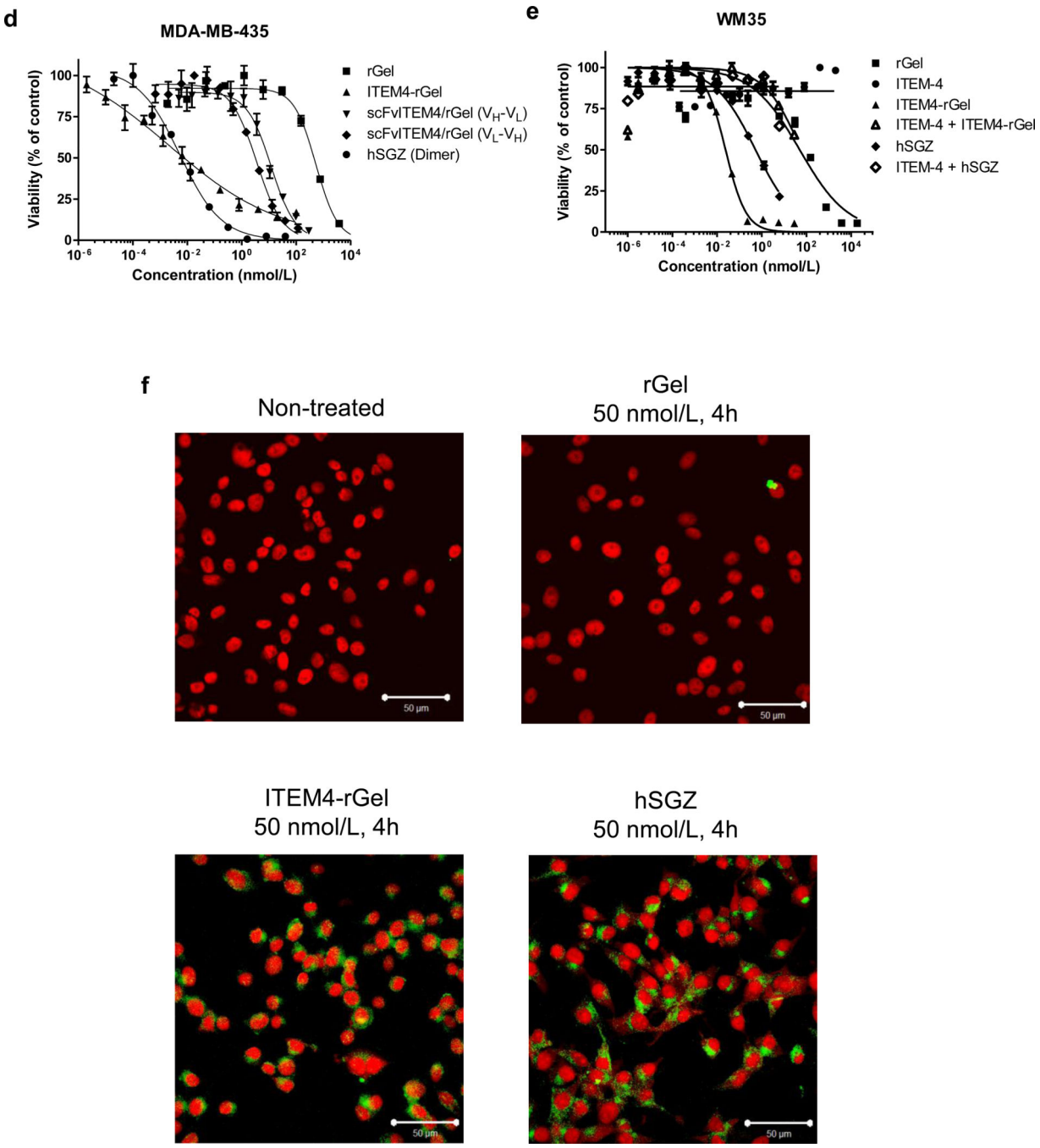

Figure 2.

Characterization of immunotoxins targeting the Fn14 receptor. **A**) Schematic diagram of immunotoxin constructs containing scFvIT4 and $_{h}$scFvIT4, peptide linker (218 and L), rGel toxin and bZIP dimerization domain. The amino acid sequence of the linker and bZIP domain is shown. **B**) SDS-PAGE analysis of purified scFvIT4 and immunotoxins in non-reducing conditions. **C**) Surface plasmon resonance analysis of scFvIT4, $_{h}$scFvIT4, ITEM-4 and immunotoxin binding to recombinant Fn14 extracellular domain. **D**) Various concentrations of rGel, ITEM4-rGel, two different formats of fusion immunotoxins, and

bivalent format of hSGZ were added to MDA-MB-435 cells and cytotoxicity was measured as described in Materials and Methods. **E**) Pretreated WM35 cells with ITEM-4 abrogated the cytotoxic effects of ITEM4-rGel and hSGZ. **F**) Internalization of ITEM4-rGel and hSGZ into MDA-MB-435 cells. Scale bar = 50 μm.

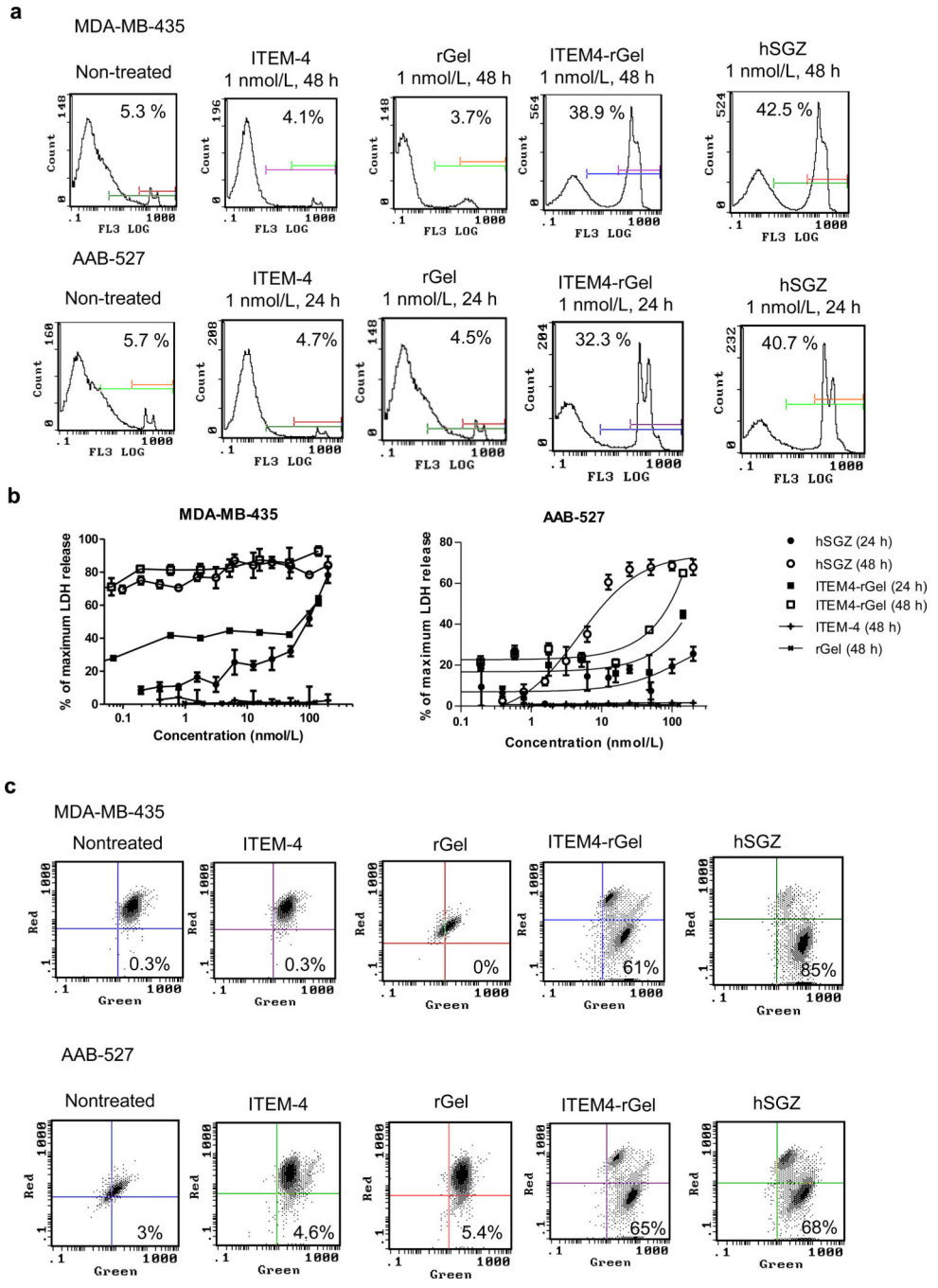

Figure 3.

Cell death induced by ITEM4-rGel and hSGZ resembles necrosis. **A**) PI exclusion assay for ITEM4-rGel and hSGZ after 48 or 24 h of exposure in MDA-MB-435 and AAB-527 cells, respectively. The percentage of cells with PI staining is indicated within each panel. **B**) LDH release assay for ITEM4-rGel and hSGZ after 24 and 48 h of treatment in MDA-MB-435 and AAB-527 cells. Results represent mean ± SD, n = 3. **C**) MDA-MB-435 and AAB527 cells were either left untreated or treated with 1 nmol/L ITEM-4, ITEM4-rGel or hSGZ for 48 h and then mitochondrial membrane depolarization was assayed by JC-1 staining

followed by flow cytometric analysis. Numbers in the lower right quadrants, percentage of cells with JC-1 green fluorescence.

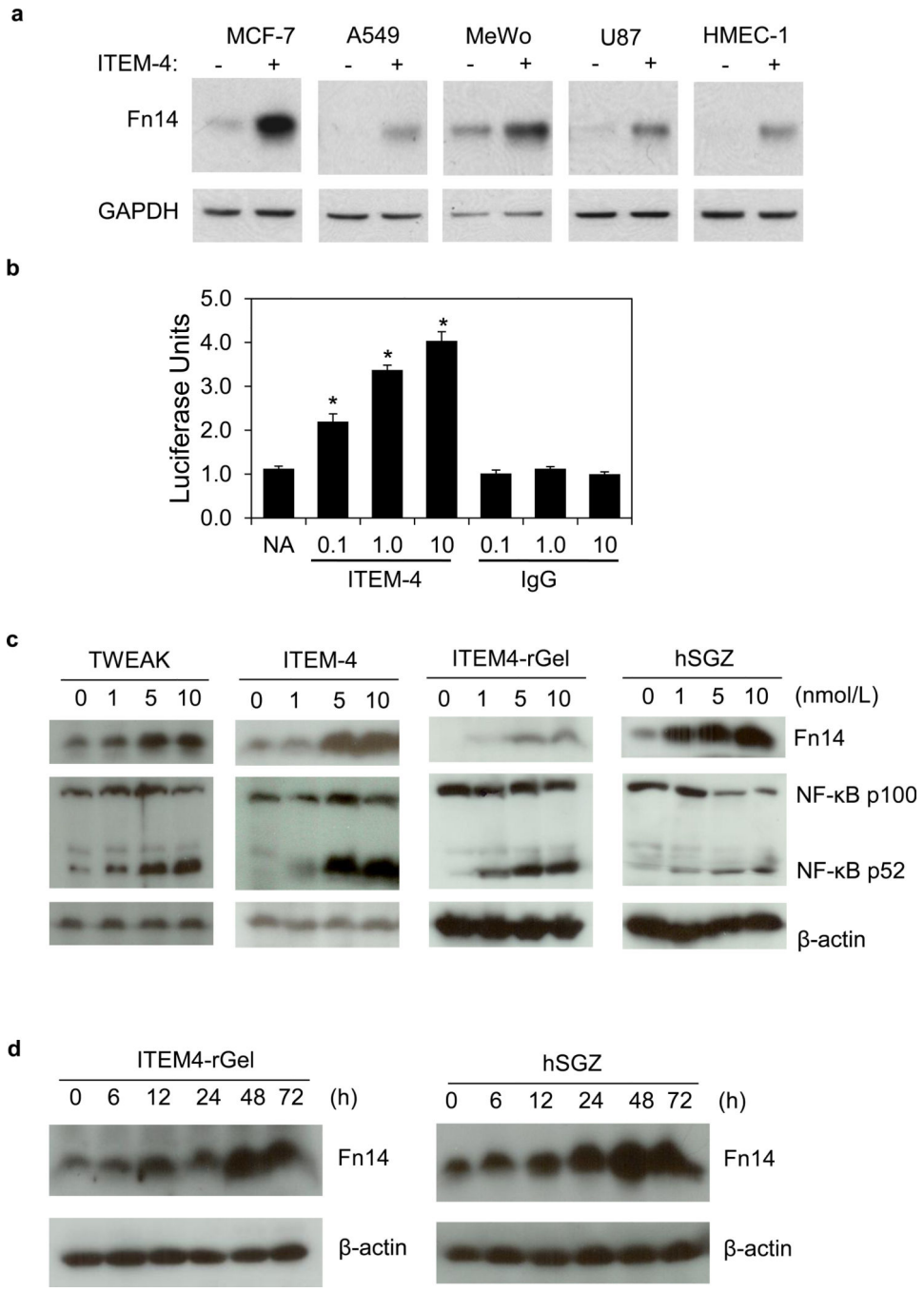

Figure 4.

ITEM4-rGel and hSGZ exhibit agonist activity. **A**) Indicated cells were either left untreated or treated with 10 Wg/ml ITEM-4 for 12 h. Fn14 or GAPDH levels were analyzed by Western blot. **B**) HEK293/NFκB-luc/Fn14 cells were either left untreated or treated with the indicated concentration of ITEM-4 or mouse IgG for 6 h. NF-κB reporter activation was measured using a luminometer. The values shown are mean ± S.D. (n=3. *, $p < 0.05$). MDA-MB-435 cells were treated with the indicated concentrations of ITEM4-rGel, hSGZ, ITEM-4 or TWEAK for 48 h (**C**) or were treated with 1 nmol/L of ITEM4-rGel or hSGZ for

the indicated time points (**D**). Cells were analyzed for Fn14, β-actin, and/or NF-κB p100 processing to p52 by Western blot.

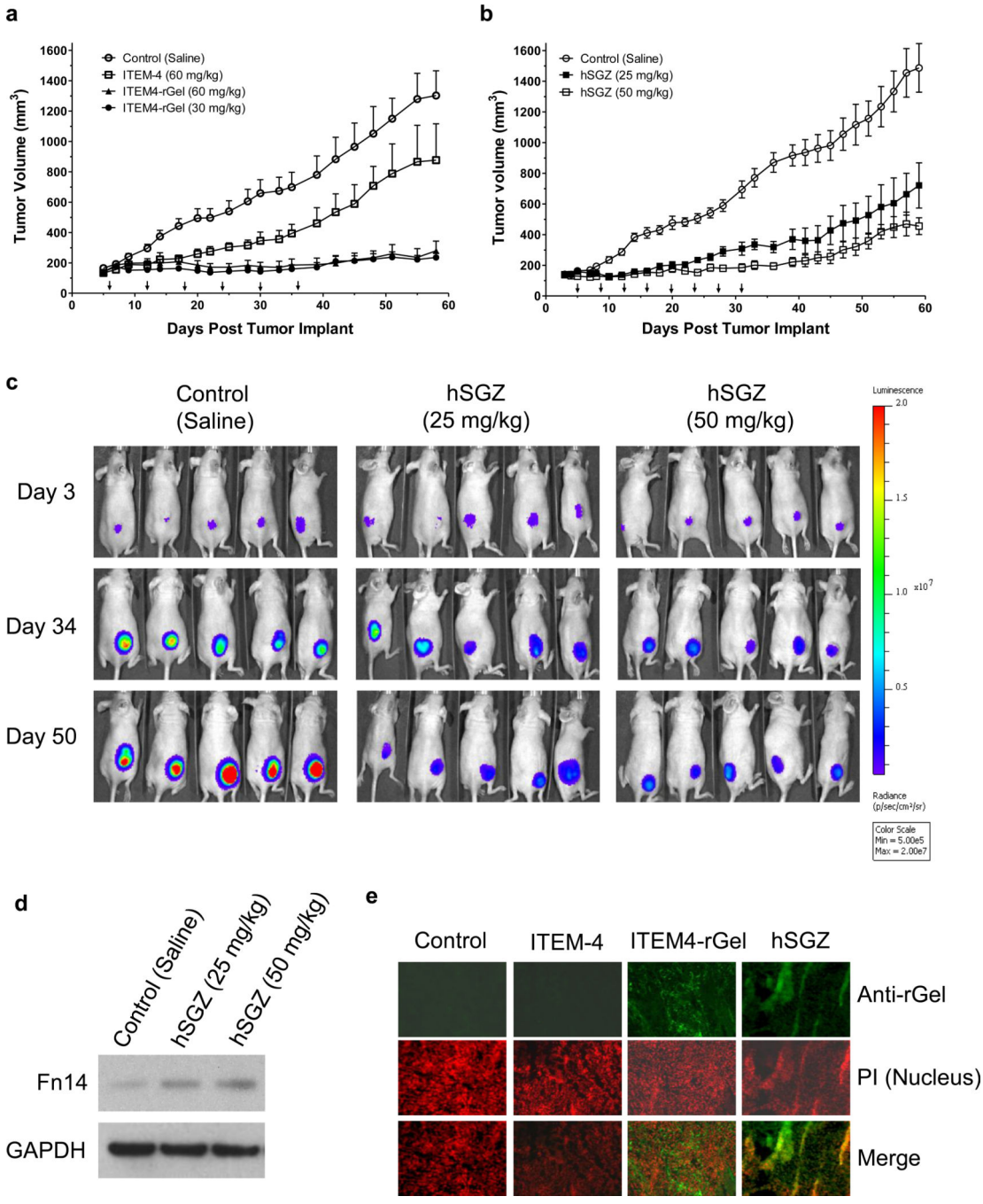

Figure 5.

Antitumor activity of Fn14-targeted immunotoxins against MDA-MB-435-LUC tumor xenografts in mice. Tumor growth during treatment (*i.v.* injection) of MDA-MB-435 flank tumors with PBS, ITEM-4 or ITEM4-rGel (**A**) or with PBS or hSGZ (**B**) on the indicated days (arrows) with the indicated total doses. For both A) and B), mean tumor volume was calculated using the formula W×L×H as measured by calipers. Data are mean ± SEM (n=5). **C**) The BLI images of tumor burden from the xenograft experiment in (B) are shown on selected days. **D**) Tumor tissues from the xenograft experiment in (B) were analyzed for

Fn14 and GAPDH expression by Western blot. **E**) Immunofluorescence staining of MDA-MB-435 tumor samples using an anti-rGel antibody after PBS, ITEM-4, ITEM4-rGel or hSGZ administration.

Table 1

Summary of the immunostaining of Fn14 across 462 samples from 169 patients with melanoma.

Specimen		IHC score				≥ 2+	Percent
		0	1+	2+	3+		
Nevus	Thin	4	1	9	21	30/35	84%
	Thick	7	7	38	35	73/87	
Primary	Thin	4	1	24	42	66/71	92%
	Thick	9	3	50	57	107/119	
Metastases	Lymph node	25	0	3	32	35/60	58%
	Visceral	38	1	7	44	51/90	

Notes: IHC score is based on the percentage of epithelial cells stained in the tumor portion of the sample: “0,” less than 5% positive cells; “1,” 5–25% positive cells; “2,” >25– 75% positive cells; “3,” greater than 75% positive cells. Thin refers to lesions <1 mm; Thick refers to lesions > 1mm.